Progress In Electromagnetics Research Letters, Vol. 18, 29–39, 2010

WIDEBAND SSN SUPPRESSION IN HIGH-SPEED PCB USING NOVEL PLANAR EBG

H.-S. He, X.-Q. Lai, Q. Ye, and Q. Wang

Institute of Electronic CAD
Xidian University
Xi'an 710071, China

W.-D. Xu

Library of Xi'an Aerotechnical College
Xi'an 710077, China

J.-G. Jiang and M.-X. Zang

Computer School
Xidian University
Xi'an 710071, China

Abstract—Simultaneous switching noise (SSN) is a significant problem in high-speed circuits. To minimize its effect and improve the electrical characteristics of circuits such as signal integrity (SI) and power integrity (PI), a novel power plane with planar electromagnetic bandgap (EBG) structure is proposed for SSN suppression in printed circuit boards (PCB) in this paper. In which a kind of improved long bridge is used and the equivalent parallel inductance can be increased significantly. Compared to the typical spiral bridge EBG structure with the same parameters, the long bridge EBG structure will change bandgap into dual-band, with lower center frequency and wider bandwith. The effectiveness and accuracy of this structure are verified by both simulations and measurements.

Received 1 August 2010, Accepted 13 September 2010, Scheduled 29 September 2010
Corresponding author: H.-S. He (hshe@live.cn).

1. INTRODUCTION

Today's very large scale integrate circuit is widely used in high-speed systems. Signal integrity (SI) problems, power integrity (PI) issues have become more and more significant in circuit design. In printed circuit boards (PCB), the integrated chips often have thousands of gates to switch in high frequency, and undesirable simultaneous switching noise (SSN) is produced, which is harmful for the PI of the circuit. Therefore, research on new effective approaches to mitigating SSN in high-speed PCB is attracting considerable attention.

As a kind of effective method for noise suppression, electromagnetic bandgap (EBG) structures has been studied very extensive. It is used in an antenna to improve the performance of the antenna for suppression of surface waves [1], such as increasing antenna gain and reducing back lobe radiation. Because of restrictions, such as size, the EBG structure has still been hardly applied to the traditional high-speed circuit.

In this paper, the research is focused on how to improve the EBG structure for 200 MHz–2 GHz SSN suppression in high-speed PCB. A novel wideband planar EBG with long bridge is put forward. This novel structure can decrease the center frequency and broaden the bandwidth of the stopband. Simulations and measurements are performed to verify the suppression of surface waves. Good performances are observed.

This paper is organized as follows. Section 2 the typical planar EBG structure with spiral bridge is briefly investigated, and its accurate equivalent circuit model is discussed. The long bridge structure is proposed and researched in Section 3. The results of simulations and measurements are given in Section 4. Lastly, the conclusions are given in Section 5.

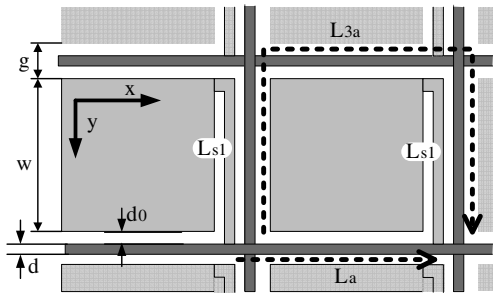

Figure 1. Survey view of a simple spiral bridge EBG structure.

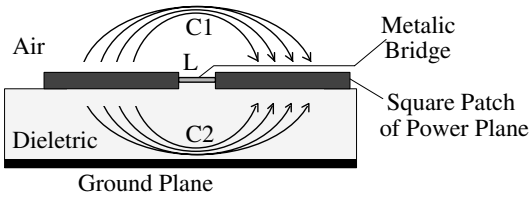

Figure 2. Section view of planar EBG structure.

2. TYPICAL PLANAR EBG STRUCTURE

A typical planar EBG with simple spiral bridge structure is known as a kind of generally used EBG structure [2], shown in Figure 1 and Figure 2. The metallic square patches are periodically distributed on the dielectric surface, and each two adjacent patches are connected by narrow metallic bridges.

The size of a typical planar EBG structure is much smaller than the wavelength. It can be analyzed by using lumped impedance parameters. When an electromagnetic wave is transmitted along x or y direction in the high impedance surface of the EBG, induced current in the metallic surface will be created and flow from a metallic patch into another by a bridge, which is equivalent to an inductor. Charge is accumulated in the adjacent patch edge, which is equivalent to a capacitor. Thus, the planar EBG structure can be simply expressed as an LC parallel equivalent circuit, where L and C are the equivalent inductor and equivalent capacitor respectively.

In the epsilon neighborhood of the center frequency, an EBG structure exhibits high impedance characteristics and suppresses transmission of any electromagnetic wave in the range of the bandgap. The equivalent capacitance C and equivalent inductance L are related to many parameters. For the square shape patch, which is commonly used as an example, the geometry parameters are denoted as ($w,\ a,\ g,\ d,\ d_0,\ t,\ t_0,\ \varepsilon_r,\ \mu_0,\ \varepsilon_0$), where w is the side of the patch unit, a is the unit cell period ($a = w + g$), g is the distance between adjacent patches, d is the width of metallic bridge, d_0 is the distance between the patch and bridge, t and ε_r are the thickness and relative permittivity of the dielectric, t_0 is thickness of the copper foil, and μ_0 and ε_0 are the magnetic permeability and permittivity in vacuum. This structure has same characteristic along both x direction and y direction. Thus, the accurate equivalent C and L can be given as follows.

(1) As shown in Figure 2, the accurate equivalent capacitance is

given by the following expression:

$$C = C_1 + C_2 \tag{1}$$

While C_1 is the gap capacitance in the air, C_2 is the gap capacitance in the dielectric. Based on the boundary property, we obtain the following [3]:

$$C_1 = \frac{\varepsilon_0 w}{\pi} \text{acosh}\left(\frac{a}{g}\right) \tag{2}$$

This equation is available for the air without boundary, but it is not suitable for the dielectric with metal ground boundary. Thus, C_2 is derived as follows:

$$C_2 = \frac{\varepsilon_0 \varepsilon_r w}{\pi} \text{acosh}\left[\frac{\sinh(\frac{\pi a}{4t})}{\sinh(\frac{\pi g}{4t})}\right] \tag{3}$$

Therefore, the total equivalent C has the following form:

$$C = \frac{\varepsilon_0 w}{\pi} \text{acosh}\left(\frac{a}{g}\right) + \frac{\varepsilon_0 \varepsilon_r w}{\pi} \text{acosh}\left\{\frac{\sinh[\frac{\pi(w+g)}{4t}]}{\sinh\left[\frac{\pi g}{4t}\right]}\right\} \tag{4}$$

(2) The main element involved in the equivalent inductance are the self inductance L_{s1} of the self bridge of each cells, and he self inductance L_{s2} of the bridge of between adjacent cells. The spiral bridge structure shown in Figure 1 is the simplest case with only one straight self bridge. Accordingly, it is assumed that the length of the self bridge is equal to w approximately. we obtain the following [4]:

$$L_{s1} = \frac{\mu_0 w}{2\pi}\left[\ln\left(\frac{w}{d+t_0}\right) + \frac{1}{2}\right] \tag{5}$$

Then, as shown in Figure 1, the L_{s2} between adjacent cells can be simply as a parallel structure with two parts, one is a bridge with a length a, and the other is a bridge with a length $3a$. The L_{s2} can be given as following:

$$\begin{aligned} L_{s2} &\approx L_a \parallel L_{3a} \\ &= \left\{\frac{\mu_0 a}{2\pi}\left[\ln\left(\frac{a}{d+t_0}\right) + \frac{1}{2}\right]\right\} \parallel \left\{3 \cdot \frac{\mu_0 a}{2\pi}\left[\ln\left(\frac{a}{d+t_0}\right) + \frac{1}{2}\right]\right\} \\ &= \frac{3}{4} \cdot \frac{\mu_0 a}{2\pi}\left[\ln\left(\frac{a}{d+t_0}\right) + \frac{1}{2}\right] \\ &= \frac{3\mu_0 a}{8\pi}\left[\ln\left(\frac{a}{d+t_0}\right) + \frac{1}{2}\right] \end{aligned} \tag{6}$$

Therefore, the total equivalent C has the following form:

$$\begin{aligned} L &= 2 \cdot L_{s1} + L_{s2} \\ &= \frac{\mu_0 w}{\pi}\left[\ln\left(\frac{w}{d+t_0}\right)+\frac{1}{2}\right]+\frac{3\mu_0 a}{8\pi}\left[\ln\left(\frac{a}{d+t_0}\right)+\frac{1}{2}\right] \end{aligned} \quad (7)$$

The parallel resonance of a perfect high impedance surface EBG is equivalent to perfect magnetic conductor (PMC). In the equivalent circuit model, the surface impedance of EBG structure is expressed by (8), where $\omega = 2\pi f$ is the angular frequency:

$$Z_{surface} = \frac{j\omega L}{1-\omega^2 LC} \quad (8)$$

Then, the stopband is determined by the lower corner frequency f_L, the upper corner frequency f_H, and the center frequency f_0. The center frequency and the relative bandwidth are given by the Equations (9) and (10) respectively [5]:

$$f_0 = \frac{f_H + f_L}{2} = \frac{1}{2\pi\sqrt{LC}} \quad (9)$$

$$\Delta BW = \frac{f_H - f_L}{f_0} = 2\frac{f_H - f_L}{f_H + f_L} \sim \sqrt{\frac{L}{C}} \cdot \sqrt{\frac{\varepsilon_0}{\mu_0}} \quad (10)$$

However, the relative bandwidth of the planar EBG structure is still not wide enough in lower frequency. This effect will be more obvious in particular when the center frequency is lower. To solve the problem, many researchers have conducted in-depth research to broaden its bandwidth by changing physical parameters. However, some drawbacks exist in these methods for SSN suppression. Physical size had to be increased and it's thus more difficult to be used in a high-speed PCB. Therefore, the primary concern is to offer larger bandwidth while controlling EBG physical size as much as possible.

3. IMPROVED LONG BRIDGE STRUCTURE

Therefore, based on the deep analysis of lumped model [6], a process for increasing series inductance is used, and the long bridge EBG structure is put forward, as shown in Figure 3.

It can be seen that an improved long bridge is used in the power plane. For increasing the inductance between the patches, this bridge is used in the gaps between each row of patches, and each row are connected with the long bridge in different side. Thus an additional series inductor will be put between adjacent patches along the x direction. Series inductance are added in traditional typical planar

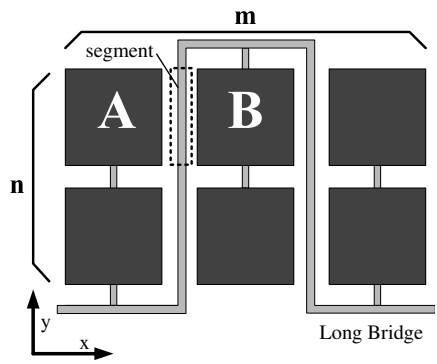

Figure 3. Long bridge structure of EBG.

EBG by the long bridge. The inductance between adjacent patches along the x direction is increased. For example, if the patches array consist of $m \times n$ unit cells (Figure 3), the long bridge in each period could be separate into one bridge with a length $n \cdot a$, and two bridges with a length $a/2$. Then, the inductance of the long bridge in each period can be given by the following expression, where u is width of the long bridge:

$$L_{u1} = \frac{na\mu_0}{2\pi}\left[\ln\left(\frac{na}{u+t_0}\right)+\frac{1}{2}\right]+\frac{a\mu_0}{2\pi}\left[\ln\left(\frac{\frac{a}{2}}{u+t_0}\right)+\frac{1}{2}\right] \qquad (11)$$

Therefore, the finally improved equivalent inductance between two adjacent patches A and B can be given as $L_{new} = (n+1)L_{s1} + L_{u1}$. And we can also use spiral bridge or L-bridge [7] or S-bridge [8] between patches in the same row to increase the inductance additionally, the center frequency of main stopband will be much lower and a wider relative bandwidth will be obtained according to Equations (9) and (10). And it can be useful for the SSN suppression which is mainly from very low frequency up to 2 GHz.

Although series inductance between adjacent patches along the straight y direction will not be increased. The size of the long bridge EBG structure will be much smaller, and we can make up a deficiency by mixed EBG with different structure direction or optimization of the circuit design.

Furthermore, because of the distribution capacitance of the long bridge, another bandgap will be produced. It can be seen that the distribution capacitance of the long bridge between patch A and patch B is a segment with the length w and width u, we can set $w' = \sqrt{wu}$, according to Equation (4), the equivalent capacitance of the new

stopband can be deduced as follows:

$$C_{new} = \frac{\varepsilon_0 w'}{\pi} \text{acosh}\left(\frac{w' + d_0}{d_0}\right) + \frac{\varepsilon_0 \varepsilon_r w'}{\pi} \text{acosh}\left\{\frac{\sinh\left[\frac{\pi(w'+d_0)}{4t}\right]}{\sinh\left[\frac{\pi d_0}{4t}\right]}\right\} \quad (12)$$

However, the inductance between patch A and the segment of long bridge and the inductance between the segment of long bridge and patch B are not equal, so the new bandgap will be produced by the overlapping of multi-band.

4. SIMULATION AND MEASUREMENT VERIFICATION

As shown in Figure 4, to demonstrate the effectiveness of the improved long bridge EBG based on the conclusion deduced in Section 3, a typical long bridge planar EBG with the direction 17.4 mm × 17.4 mm consisting of 6 × 6 unit cells is designed as a reference. The substrate dielectric is FR4 with a relative permittivity of 4.4 and a loss tangent of 0.02. The thickness of the substrate is 0.4 mm and the thickness of the copper foil t_0 is 0.035 mm. The corresponding parameters are $w = 2.5$ mm, and $g = 0.4$ mm. Then, two kind of planar EBG with the long bridge was fabricated with the width of the long bridge $u = d = 0.1$ mm and the the distance $d_0 = 0.15$ mm. One uses straight bridge between patches in each row (Figure 6), the other uses L shape bridge between patches in each row with the length w. All the width of L-bridge and straight bridge are the same.

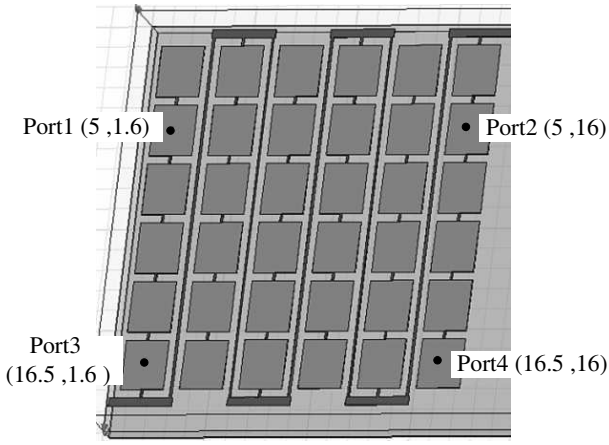

Figure 4. EBG isolation test for SSN suppression.

Finally, for the reference, a spiral bridge EBG mentioned in Figure 1 is also fabricated with the same parameters, but the width should be $w' = 2.4\,\text{mm}$, and the the distance should be $d'_0 = 0.1\,\text{mm}$, $g'_0 = 0.3\,\text{mm}$ in x direction. So the period a of these EBG structures are the same. According to all the equations above,we can conclude the following results in Table 1.

Finite element analysis (Ansoft HFSS) are performed after calculation, the simulated S parameters (S_{21}, S_{43}, S_{41}) of the three different structures can be obtained, which are shown in Figures 5–7.

From the curves shown in Figure 5, as $-30\,\text{dB}$ as the measure standard,the single stopband of the typical spiral bridge planar EBG structure is ranging from 5.8 to 7.9 GHz, but from the curves shown in Figure 6 and Figure 7, the long bridge structure has dual stopband, and the results are all given in Table 2.

Table 1. Calculation result of main bandgap.

	C (pF)	L (nH)	f_0 (GHz)	$\sqrt{L/C} \cdot \sqrt{\varepsilon_0/\mu_0}$
Long bridge (with straight bridge)	0.135	21.204	2.973	1.051
Long bridge (with L-bridge)	0.135	32.282	2.41	1.297
Traditional (with spiral bridge)	0.112	4.97	6.32	0.511

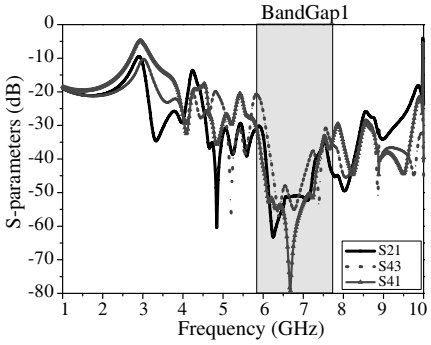

Figure 5. Simulated S parameters of spiral bridge EBG structures.

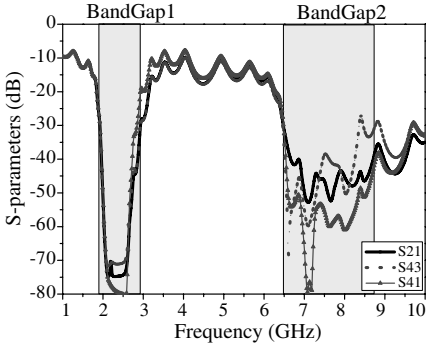

Figure 6. Simulated S parameters of long bridge EBG structures with straight bridge in each row.

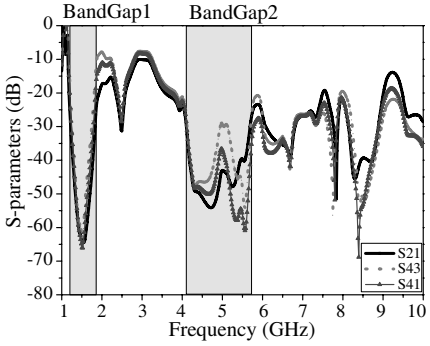

Figure 7. Simulated S parameters of long bridge EBG structures with L-bridge in each row.

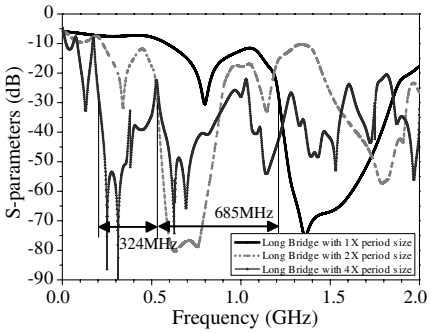

Figure 8. Measured S parameters of long bridge EBG structures with L-bridge in each row.

Table 2. Test results.

	f_L (GHz)	f_H (GHz)	f_0 (GHz)	BW (GHz)	ΔBW
Traditional (with spiral bridge)	5.8	7.9	6.85	2.1	30.7%
Long bridge	1.92	2.92	2.42	1	41.6%
(with straight bridge)	6.48	8.86	7.67	2.38	31%
long bridge	1.22	1.82	1.52	0.6	39.5%
(with L-bridge)	4.1	5.69	4.9	1.59	32.4%

From Table 2, we can see the simulation results of bandgap 1 of each structure are closely matching the calculation results in Table 1. The center frequency f_0 of main stopband is decreased from 6.85 GHz to 2.42 GHz and 1.52 GHz, and the relative bandwidth is increased from 30.7 % to 41.6% and 39.5%, which is approximately 130% increase. And it also can be observed that the total bandgap of the spiral bridge EBG is 2.1 GHz, and the total bandgap of the long bridge structure are 3.38 GHz (straight bridge) and 2.19 GHz (L-bridge) respectively, that means both the relative bandwidth and the total bandwidth are increased with a lower center frequency. If it is optimized, bandgap characteristics can be further improved.

Finally, to verify the availability of the long bridge structure, a test board with the parameters mentioned above is made, with the L-bridge between patches in each row. Then another two boards with

twice period size ($w = 5\,\text{mm}$, $g = 0.8\,\text{mm}$, $u = d = 0.2\,\text{mm}$, and $d_0 = 0.3\,\text{mm}$) and four times period size ($w = 10\,\text{mm}$, $g = 1.6\,\text{mm}$, $u = d = 0.4\,\text{mm}$, and $d_0 = 0.6\,\text{mm}$) are also made, and the low frequency comparison of measured results for are given in Figure 8. As can be seen, the measured S_{21} filtering characteristic are in good agreement with the simulation results in Figure 7, and the center frequency will be much lower when the period size increases, the lower corner frequency can be nearly 200 MHz while the period size of unit cell increased to four times. The stopband can cover 200 MHz–2 GHz frequency with much smaller structure size than the structure size ($a = 30\,\text{mm}$)in [7, 8]. Consequently, it needs smaller room and cause lesser SI problem, these are very useful for low frequency noise suppression, and the long bridge EBG structure can be implemented in real applications for power noise suppression and DC IR drop.

5. CONCLUSION

In this paper, a novel compact planar EBG structure with long bridge is presented for SSN suppression. Compared to the typical planar EBG with spiral bridge structure with the same period size, the long bridge structure can produce dual stopband, and increases the relative bandwidth to nearly 130%, with a significant decrease of the center frequency of the both two stopband. And the center frequency will be much lower when the period size increases. It is not only an effective method for improving the bandwidth of the EBG structure, but also an effective isolation structure which can overcome the drawback of planar EBG. The unit can also be optimized by mixed with spiral bridge or ferrite film [9] or high-k dielectrics [10] to gain better suppression ripples. Therefore, the long bridge structure is very useful for SSN suppression in high-speed PCB. It's a structure that provides a very effective solution for noise suppression in the range of GHz applications.

ACKNOWLEDGMENT

This work was supported by Key Lab of High-speed Circuit Design and EMC, Ministry of Education in China.

REFERENCES

1. Mahdi Moghadasi, S., A. R. Attari, and M. M. Mirsalehi, "Compact and wideband 1-D mushroom-like EBG filters," *Progress In Electromagnetics Research*, Vol. 83, 323–333, 2008.

2. Genovesi, S. and A. Monorchio, "A novel electromagnetic bandgap structure for broadband switching noise suppression in high-speed printed circuit boards," *Proceedings of the 38th European Microwave Conference*, 1374–1377, October 2008.
3. Yanagi, T., T. Oshima, H. Oh-hashi, Y. Konishi, S. Murakami, K. Itoh, and A. Sanada, "Lumped-element loaded EBG structure with an enhanced bandgap and homogeneity," *Proceedings of iWAT2008*, 458–461, 2008.
4. Young, B., *Digital Signal Integrity Modeling and Simulation with Interconnects and Packages*, Prentice Hall, October 19, 2000.
5. Zhang, M.-S., Y.-S. Li, C. Jia, and L.-P. Li, "Signal integrity analysis of the traces in electromagnetic-bandgap structure in high-speed printed circuit boards and packages," *IEEE Transactions on Microwave Theory and Techniques*, Vol. 55, No. 5, 1054–1062, May 2007.
6. Kamgaing, T. and O. M. Ramahi, "Design and modeling of high-impedance electromagnetic surfaces for switching noise suppression in power planes," *IEEE Transactions on Electromagnetic Compatibility*, Vol. 47, No. 3, 479–489, Aug. 2005.
7. Wu, T.-L., C.-C. Wang, Y.-H. Lin, T.-K. Wang, and G. Chang, "A novel power plane with super-wideband elimination of ground bounce noise on high speed circuits," *IEEE Microwave and Wireless Components Letters*, Vol. 15, No. 3, 174–176, March 2005.
8. Joo, S.-H., D.-Y. Kim, and H.-Y. Lee, "A S-bridged inductive electromagnetic bandgap power plane for suppression of ground bounce noise," *IEEE Microwave and Wireless Components Letters,* Vol. 7, No. 10, 709–711, October 2007.
9. Toyota, Y., K. Kondo, S. Yoshida, K. Iokibe, and R. Koga, "Stopband characteristics of planar-type electromagnetic bandgap structure with ferrite film," *2010 Asia-Pacific International Symposium on Electromagnetic Compatibility*, 664–667, April 12–16, 2010.
10. Mohajer-Iravani, B. and O. M. Ramahi, "Suppression of EMI and electromagnetic noise in packages using embedded capacitance and miniaturized electromagnetic bandgap structures with high-k dielectrics," *IEEE Transactions on Advanced Packing*, Vol. 30, No. 4, 776–788, November 2007.